

(1) Electrochemical performance comparison:

We have summarized the recently reported results on the electrochemical performance of metal-single atoms in liquid/solid-state lithium-sulfur (Li-S) batteries in **Table R1 and Figure R1**. It is evident that although many reports demonstrate seemingly excellent electrochemical performance, they often lack a comprehensive evaluation of performance metrics, including the sulfur content in the battery, the cathode-to-anode ratio (N/P), and the overall energy density of the battery. The introduction of inactive materials can significantly reduce the overall energy density of the battery.

Our self-supporting, ultra-lightweight FeCFs, with their integrated design and superior conductivity and catalytic effect towards LPSs, exhibit a very high sulfur content (~90%). Additionally, our FeCFs also serve as an excellent lithium metal host. There are few reports on the modification effects of single-atom host materials on lithium-metal anodes. As shown in **Figure R1(c)**, our FeCFs@Li can cycle for over 10,000 hours, and it exhibits very low overpotential even at a charge/discharge current density of 8 mA cm⁻². Thus, the assembled pouch cells demonstrate excellent electrochemical performance, with an energy density approaching 400 Wh kg⁻¹. As illustrated in **Figure R1 (a,b)**, our uniquely designed FeCFs@S//pDOL//FeCFs@Li lithium-sulfur full cell device exhibits electrochemical performance that is on par with or superior to both liquid and solid-state Li-S batteries.

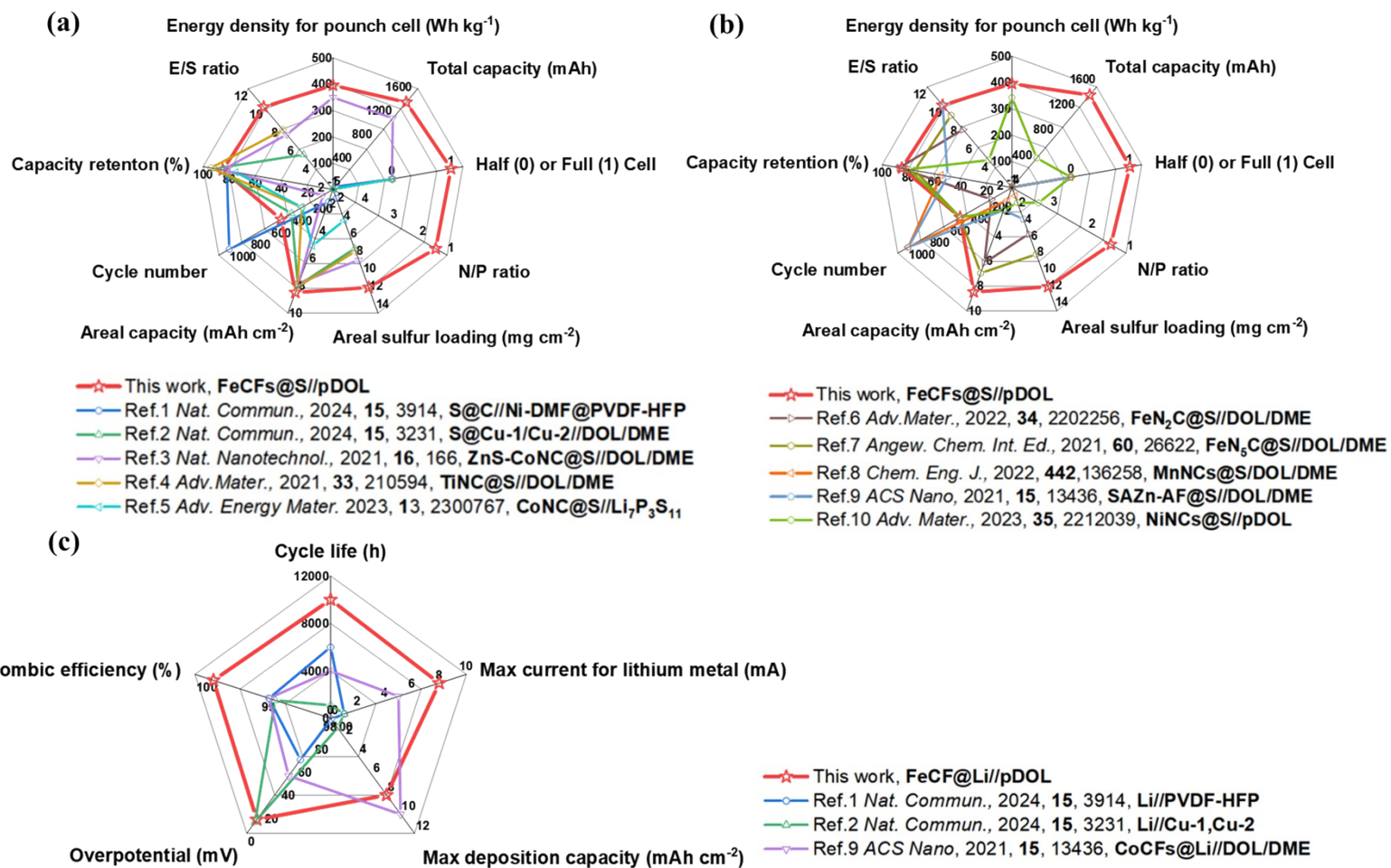


Figure R1 (a-c) The electrochemical performance of solid-state Li-S batteries based on single-metal atom composite materials in this work is compared with the performance of metal single-atom materials reported in recent literature for liquid/solid Li-S batteries (a, b) and in Li-S batteries and lithium-metal anodes (c).

Table R1. The electrochemical performance of solid-state Li-S batteries based on single-metal atom composite materials in this work is compared with the performance of metal single-atom materials in liquid/solid-state Li-S batteries reported in recent literature, including metrics such as electrode sulfur loading, cycle number, and areal capacity.

| | This work | Ref.1 | Ref.2 | Ref.3 | Ref.4 | Ref.5 | Ref.6, | Ref.7 | Ref.8 | Ref.9 | Ref.10 |
|--|------------------|--------------|--------------|--------------|--------------|--------------|---------------|--------------|--------------|--------------|---------------|
| Pouch Cell specific energy (Wh kg⁻¹) | 396 | - | - | 350 | - | - | - | - | - | - | 343 |
| Capacity (mAh) | 1470 | 47 | 8.2 | 1200 | 10 | 6 | 6 | 7 | 2 | 2 | 470 |
| Half (0) or Full (1) Cell | 1 | 0 | 0 | 0 | 0 | 0 | 0 | 0 | 0 | 0 | 0 |
| N/P ratio | 1.4 | - | - | - | - | - | - | - | - | - | 3.3 |
| Areal sulfur loading (mg cm⁻²) | 12.1 | 2 | 7.7 | 9 | 8 | 4.5 | 5.75 | 8.2 | 1.2 | 4 | 2 |
| Area capacity (mAh cm⁻²) | 8.5 | 1.9 | 8 | 7.8 | 8.1 | 5.1 | 6.18 | 7 | 1.2 | 2 | 2 |
| Cylce life for Li-S batteries | 500 | 1000 | 400 | 100 | 300 | 300 | 200 | 500 | 1000 | 1000 | 500 |
| Capacity retention (%) | 85 | 81.9 | 91.3 | 85.2 | 94 | 75 | 87 | 75.2 | 55 | 50 | 80 |
| E/S ratio* | 10 | - | 4.8 | 7 | 7.5 | - | 7.35 | 8.9 | - | 10 | 4 |
| Sulfur content (%) | 90 | 40 | 78.8 | - | 65 | 40 | 83 | - | 85 | - | 60 |

* The E in E/S in this work is based on the mass of the DOL/LiTFSI used before *in-situ* polymerization.

(2) Descriptor model comparison:

We have summarized the descriptors used for lithium polysulfides (LPSs) adsorption and conversion in Li-S batteries from recent reports, along with their characteristics. The results are presented in **Figure R2** and **Table R2**. It is evident that employing a unified descriptor to rationally describe the complex LPSs conversion kinetics in Li-S batteries is a goal pursued by many researchers. However, almost all proposed descriptors are often limited to specific models, and their transferability has not been validated. With the introduction of machine-learning (ML) algorithms, this situation has somewhat improved. However, the models obtained through machine learning lack physical interpretability and cannot deeply reveal the physical factors influencing polysulfide conversion. Furthermore, the descriptors reported in current literature generally describe only the adsorption energy of LPSs, often neglecting the conversion energy barriers of LPSs and the decomposition energy barriers of the discharge product Li_2S .

Our new descriptor, based on a *d-p* coupling model and incorporating machine-learning algorithms with electronic/atomic geometric structure factors, can effectively provide a unified description of LPSs adsorption, conversion, and the decomposition energy barriers of the discharge product Li_2S . Additionally, this descriptor can accurately describe the LPSs conversion effectiveness in models other than single atoms, revealing the influence of the valence electrons of metals and non-metals on LPSs conversion kinetics. Furthermore, the proposed descriptor in this work also achieves a synergistic integration of machine-learning algorithms, physical models,

and experimental results. This approach provides a new research paradigm for achieving high-performance Li-S batteries in the future.

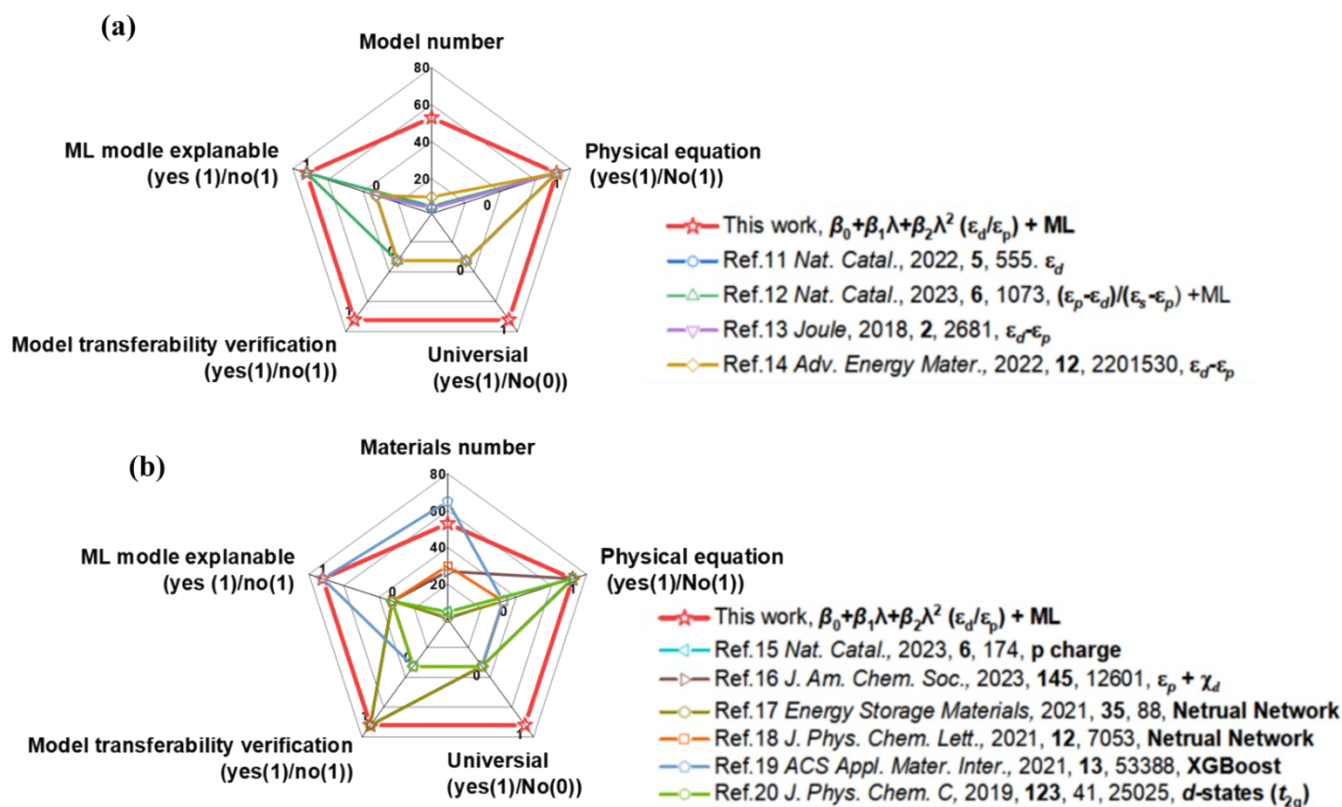


Figure R2. (a,b) Comparison of universality and transferability of the model constructed with the assistance of machine-learning algorithms in this work and the models reported in recent reports to describe the catalytic conversion kinetics of LPSs in Li-S batteries

Table R2. Comparing results of the uniqueness and generalizability of descriptors describing LPSs conversion kinetics in Li-S batteries between this work and recently published papers.

| | This work | Ref.11 | Ref.12 | Ref.13 | Ref.14 | Ref.15 | Ref.16 | Ref. 17 | Ref.18 | Ref.19 | Ref.20 |
|--|---|-----------------|--|---------------------------------|---------------------------------|------------|--------------------------|----------------|----------------|---------|-------------|
| Materials_number | 53 | 4 | 5 | 4 | 10 | 5 | 27 | 2 | 30 | 65 | 5 |
| Physical equation (yes (1)/no (0)) | 1 | 1 | 1 | 1 | 1 | 1 | 1 | 0 | 0 | 0 | 1 |
| E_LPSs_binding (yes(1)/no(1)) | 1 | 1 | 1 | 0 | 1 | 0 | 1 | 1 | 1 | 1 | 0 |
| E_Li₂S_decomposition (yes (1)/no (0)) | 1 | 0 | 1 | 0 | 1 | 0 | 0 | 0 | 0 | 0 | 0 |
| LPSs_conversion_path (yes (1)/no (0)) | 1 | 1 | 0 | 0 | 1 | 0 | 1 | 0 | 0 | 0 | 0 |
| Gibbs_energy_LPSs (yes (1)/no (0)) | 1 | 0 | 0 | 1 | 1 | 1 | 1 | 0 | 0 | 0 | 0 |
| Model transferability verification (yes (1)/no (0)) | 1 | 0 | 0 | 0 | 0 | 0 | 1 | 1 | 0 | 0 | 0 |
| ML_Algrithms_explana ble (yes (1)/no (0)) | 1 | - | 1 | - | - | - | - | 0 | 0 | 1 | - |
| ML_modle_explanable (yes (1)/no (0)) | Quadratic polynomial algorithm | - | Solving coefficients | - | - | - | - | Neural Network | Neural Network | XGBoost | - |
| Physical equation | $\lambda = \varepsilon_d/\varepsilon_p$ | ε_d | I(band), I(latt) | $\varepsilon_d - \varepsilon_p$ | $\varepsilon_d - \varepsilon_p$ | p charge | $\varepsilon_p + \chi_d$ | - | - | - | d -states |
| Descriptors | $\beta_0 + \beta_1\lambda + \beta_2\lambda^2$ | ε_d | Genetic Algorithm + Monte Carlo Simulation | $\varepsilon_d - \varepsilon_p$ | $\varepsilon_d - \varepsilon_p$ | p charge | $\varepsilon_p + \chi_d$ | - | - | - | t_{2g} |

Reference:

1. Y. Zhu, Z. Lao, M. Zhang, T. Hou, X. Xiao, Z. Piao, G. Lu, Z. Han, R. Gao, L. Nie, X. Wu, Y. Song, C. Ji, J. Wang and G. Zhou, *Nat. Commun.*, 2024, **15**, 3914.
2. Q. Yang, J. Cai, G. Li, R. Gao, Z. Han, J. Han, D. Liu, L. Song, Z. Shi, D. Wang, G. Wang, W. Zheng, G. Zhou and Y. Song, *Nat. Commun.*, 2024, **15**, 3231.
3. C. Zhao, G.-L. Xu, Z. Yu, L. Zhang, I. Hwang, Y.-X. Mo, Y. Ren, L. Cheng, C.-J. Sun, Y. Ren, X. Zuo, J.-T. Li, S.-G. Sun, K. Amine and T. Zhao, *Nat. Nanotechnol.*, 2021, **16**, 166.
4. Z. Han, S. Zhao, J. Xiao, X. Zhong, J. Sheng, W. Lv, Q. Zhang, G. Zhou and H.-M. Cheng, *Adv. Mater.*, 2021, **33**, 2105947.
5. H. Zhong, Y. Su, Y. Wu, J. Gu, R. Ma, Y. Luo, H. Lin, M. Tao, J. Chen, Z. Liang, K. Wang, X. Zheng, Z. Chen, J. Peng, Z. Lv, Z. Gong, J. Huang and Y. Yang, *Adv. Energy Mater.*, 2023, **13**, 2300767.
6. Y. Ding, Q. Cheng, J. Wu, T. Yan, Z. Shi, M. Wang, D. Yang, P. Wang, L. Zhang and J. Sun, *Adv. Mater.*, 2022, **34**, 2202256.
7. Y. Zhang, J. Liu, J. Wang, Y. Zhao, D. Luo, A. Yu, X. Wang and Z. Chen, *Angew. Chem. Int. Ed.*, 2021, **60**, 26622.
8. S. Qiao, D. Lei, Q. Wang, X. Shi, Q. Zhang, C. Huang, A. Liu, G. He and F. Zhang, *Chem. Eng. J.*, 2022, **442**, 136258.
9. C.-L. Song, Z.-H. Li, L.-Y. Ma, M.-Z. Li, S. Huang, X.-J. Hong, Y.-P. Cai and Y.-Q. Lan, *ACS Nano*, 2021, **15**, 13436.
10. X. Meng, Y. Liu, Y. Ma, Y. Boyjoo, J. Liu, J. Qiu and Z. Wang, *Adv. Mater.*, 2023, **35**, 2212039.
11. Z. Shen, X. Jin, J. Tian, M. Li, Y. Yuan, S. Zhang, S. Fang, X. Fan, W. Xu, H. Lu, J. Lu and H. Zhang, *Nat. Catal.*, 2022, **5**, 555.
12. Z. Han, R. Gao, T. Wang, S. Tao, Y. Jia, Z. Lao, M. Zhang, J. Zhou, C. Li, Z. Piao, X. Zhang and G. Zhou, *Nat. Catal.*, 2023, **6**, 1073.
13. J. Zhou, X. Liu, L. Zhu, J. Zhou, Y. Guan, L. Chen, S. Niu, J. Cai, D. Sun, Y. Zhu, J. Du, G. Wang and Y. Qian, *Joule*, 2018, **2**, 2681.
14. N. Gong, X. Hu, T. Fang, C. Yang, T. Xie, W. Peng, Y. Li, F. Zhang and X. Fan, *Adv. Energy Mater.*, 2022, **12**, 2201530.
15. W. Hua, T. Shang, H. Li, Y. Sun, Y. Guo, J. Xia, C. Geng, Z. Hu, L. Peng, Z. Han, C. Zhang, W. Lv and Y. Wan, *Nat. Catal.*, 2023, **6**, 174.
16. M. Fang, J. Han, S. He, J.-C. Ren, S. Li and W. Liu, *J. Am. Chem. Soc.*, 2023, **145**, 12601.
17. H. Zhang, Z. Wang, J. Ren and J. Liu, *Energy Storage Mater.*, 2021, **35**, 88.
18. Z. Lian, M. Yang, F. Jan and B. Li, *J. Phys. Chem. Lett.*, 2021, **12**, 7053.
19. H. Zhang, Z. Wang, J. Cai, S. Wu and J. Li, *ACS Appl. Mater. Interfaces*, 2021, **13**, 53388.
20. Z. Chen, W. Lv, F. Kang and J. Li, *J. Phys. Chem. C*, 2019, **123**, 25025.